Article

Journal of
Nanoscience and Nanotechnology
Vol. 16, 10558–10562, 2016
www.aspbs.com/jnn

Copyright © 2016 American Scientific Publishers
All rights reserved
Printed in the United States of America

Enhanced Cycling Properties of Carbon-Coated SnO_2–Co_3O_4 Composite Nanowires for Lithium-Ion Batteries

Bon-Ryul Koo[1], Dae-Hyeok Lee[2], Hyo-Jin Ahn[1,*], and Yung-Eun Sung[2,*]

[1] *Department of Materials Science and Engineering, Seoul National University of Science and Technology, Seoul 139-743, Republic of Korea*
[2] *School of Chemical and Biological Engineering, Seoul National University, Seoul 151-742, Republic of Korea*

Carbon-coated SnO_2–Co_3O_4 composite nanowires (NWs) are synthesized to improve the cycling properties of lithium-ion batteries, using electrospinning followed by carbonization using a dopamine precursor. These carbon-coated composite NWs show excellent capacity retention (~542 mAh/g; 50 cycles) compared to bare SnO_2 NWs (~101 mAh/g; 50 cycles) and SnO_2–Co_3O_4 composite NWs (~323 mAh/g; 50 cycles). The performance improvement is due to the combined effects of the composite structure of SnO_2 and Co_3O_4 producing the enhanced capacity retention in the NW core region and the carbon coating in the shell region hindering large volume expansion-contraction of the electrode.

Delivered by Ingenta to: Universiteit Utrecht
IP: 131.211.201.60 On: Wed, 16 Nov 2016 04:46:14
Copyright: American Scientific Publishers

Keywords: SnO_2, Lithium-Ion Batteries, Composite Nanostructure, Electrochemical Performance.

1. INTRODUCTION

Lithium-ion batteries (LIBs) are widely used in electronic applications such as mobile phones, lap-top computers and electrical vehicles requiring efficient energy storage. LIBs have high energy density (>150 Wh/kg), high operating voltage (>3.6 V), excellent cyclic performance (>1,000 cycles) and low toxicity.[1,2] Typically, LIBs consist of an anode, cathode, separator and electrolyte; the anode directly affects the electrochemical performance. Much effort has been devoted to developing anode materials with improved performance in the areas of capacity, cycleability and charge/discharge-rate. Carbon-based materials (graphite, graphene and carbon nanofibers (CNF)), lithium alloys materials (LiSi, LiSb and LiSn), transition metal-oxide materials (Fe_2O_3, NiO and Co_3O_4) and Sn- or Si-based materials (SnO_2, SnO, Si and SiO) have been investigated.[1] In particular, SnO_2 materials have been proposed to replace commercial graphite because they possesses high specific capacity (781 mAh/g for SnO_2), low potential for Li^+ intercalation and low-cost.[3,4] Nevertheless, practical application of these materials is still limited by their poor capacity retention during cycling due to the large volume expansion-contraction (~300%) of the electrodes.[3,4] To solve this problem, researchers have proposed various strategies including various nanostructure morphologies, carbon or ceramic coating, N or B doping and metal or metal-oxide composites.[5,6] For example, Park et al. reported that SnO_2 NWs can provide higher reaction sites and faster charge transfer compared to SnO_2 nanoparticles, resulting in decreased capacity loss for LIBs.[7] Kim et al. demonstrated that $AlPO_4$-coated SnO_2 particles have enhanced capacity retention (~44%, 15 cycles) compared to bare SnO_2 particles.[8] Choi et al. synthesized Janus-structured SnO_2–CuO composite nanorods using flame spray pyrolysis that showed good cyclic performance (~392 mAh/g, 50 cycles) for LIBs.[9] However, development of a novel electrode fabricated using SnO_2–Co_3O_4 composite NWs with a carbon coating has not been reported before.

We synthesized carbon-coated SnO_2–Co_3O_4 composite NWs using electrospinning followed by carbonization and investigated the correlation between the electrode structural properties and electrochemical performance. In addition, we employed dopamine as the carbon precursor because it forms a uniform and continuous carbon

*Authors to whom correspondence should be addressed.

1533-4880/2016/16/10558/005 doi:10.1166/jnn.2016.13194

layer using a simple process.[10] Unlike other precursors for a carbon coating, such as glucose, sucrose and pyrrole, dopamine allows control of the thickness by adjusting the polymerization time or dopamine concentration, a useful feature for design and optimization of electrode materials.[10]

2. EXPERIMENTAL DETAILS

Bare SnO_2 NWs, SnO_2–Co_3O_4 composite NWs and carbon-coated SnO_2–Co_3O_4 composite NWs were synthesized using electrospinning. First, the precursor solution for synthesizing bare SnO_2 NWs was prepared by dissolving tin(II) chloride dihydrate ($SnCl_2 \cdot 2H_2O$, Aldrich) and poly(vinylpyrrolidone) (PVP, $M_w = 1{,}300{,}000$ g/mol, Aldrich) in a solvent (1:1 v/v) of *N*, *N*-dimethylformamide (C_3H_7NO, DMF, Aldrich) and ethanol (C_2H_6O, Aldrich). For the SnO_2–Co_3O_4 composite NWs, cobalt(II) acetate tetrahydrate ($((C_2H_3O_2)_2Co \cdot 4H_2O$, Aldrich) was added to this solvent mixture. At this time, the weight ratio of Sn and Co precursors was adjusted to 1:1. After stirring, the dissolved mixture was loaded into an electrospinning apparatus consisting of a syringe equipped with a 23-gauge stainless steel needle, with 9.5 kV applied between the needle tip and a collector at a distance of 15 cm. The feeding rate was controlled at 0.02 mL/h. The as-prepared nanofibers were calcined at 500 °C for 5 h to obtain bare SnO_2 NWs and SnO_2–Co_3O_4 composite NWs. To synthesize a carbon coating on SnO_2–Co_3O_4 NWs, the NWs were dispersed in tris-buffer (pH: ~ 8.5) by ultrasonication for 0.5 h; dopamine used as the carbon precursor was then added to the solution. The resultant precipitates were collected by centrifugation, washed several times with deionized water and dried in a 60 °C oven for 12 h. Afterwards, the resultant sample was carbonized at 400 °C for 2 h under an Ar atmosphere and then further carbonized at 600 °C for 3 h, completing the synthesis.

The morphological properties of all samples were observed using field-emission scanning electron microscopy (FESEM, Hitachi S-4800) and transmission electron microscopy (MULTI/TEM; Tecnai G^2, KBSI Gwangju Center), respectively. The crystal structures and chemical bonding states of the samples were investigated by X-ray diffraction (XRD, Rigaku X-ray diffractometer) and X-ray photoelectron spectroscopy (XPS, ESCALAB 250 equipped with an Al K_α X-ray source). Electrochemical performance was evaluated using a Li coin cell (CR2016, Hohsen Corporation) fabricated with the as-prepared samples as anode, Li metal foil as cathode, 1.0 M $LiPF_6$ solution in ethylene carbonate (EC)/diethyl carbonate (DEC) (1:1 v/v) as electrolyte and a polypropylene membrane as separator. The anode was fabricated by mixing the active materials (70 wt%), Super *P* (10 wt%) as a conducting agent and poly(vinylidene fluoride) (20 wt%) (Alfa Aesar) as a binder in *N*-methyl-2-pyrrolidinone (NMP, Aldrich), which was coated onto a copper foil using a doctor blade. The Li coin cells were assembled in an argon-filled glove box. The electrochemical performance of all samples was determined using a WBCS 3000 battery cycler system (WonATech Corp., Korea) at a current density of 100 mA/g in a voltage range of 0.01–2.0 V (versus Li/Li^+) at 25 °C in an incubator.

3. RESULTS AND DISCUSSION

Figures 1(a–c) show FESEM images of bare SnO_2 NWs, SnO_2–Co_3O_4 composite NWs and carbon-coated SnO_2–Co_3O_4 composite NWs, demonstrating successful formation of continuous one-dimensional NWs. Bare SnO_2 NWs and SnO_2–Co_3O_4 composite NWs consist of fine grains with a rough surface. Grains of SnO_2–Co_3O_4 composite NWs are much smaller than those of bare SnO_2 NWs due to the composite structure of tin oxide and cobalt oxide. That is, SnO_2 and Co_3O_4 phases coexisted in nanostructure lead to the inhibitive grain growth of SnO_2–Co_3O_4 composite NWs, which can improve the cycling performance of LIBs.[10–12] The sample diameters are 115.3–131.4 nm for bare SnO_2 NWs, 126.6–143.7 nm for SnO_2–Co_3O_4 composite NWs and 241.6–280.1 nm for carbon-coated SnO_2–Co_3O_4 composite NWs. The carbon-coated composite NWs have a larger diameter than bare SnO_2 and SnO_2–Co_3O_4 composite NWs, implying that carbon layers were successfully coated onto the composite NWs.

Delivered by ingenta to: Universiteit Utrecht
IP: 131.211.80.252 On: Wed, 13 Apr 2016 04:46:14
Copyright: American Scientific Publishers

To further investigate the structure of carbon-coated SnO_2–Co_3O_4 composite NWs, TEM analyses were carried out. Figure 2 shows TEM images obtained from the carbon-coated SnO_2–Co_3O_4 composite NWs, which are composed of a core appearing as a dark region and a shell which appears lighter. That is, the core region consists of small nanoparticles (4.9–6.3 nm in size) corresponding to SnO_2 and aggregations (42.8–80.9 nm in size) corresponding to Co_3O_4. For the shell region, the TEM image appears bright-grey in contrast to the carbon which has an amorphous structure. The carbon layer in Figure 2(b) is in the range of 56.3–59.1 nm thick. To investigate the elemental distribution, TEM-EDS mapping of the carbon-coated SnO_2–Co_3O_4 composite NWs was performed. Figure 2(c) shows that Co atoms are partially aggregated in the NWs and Sn atoms are well dispersed. Also, it is observed that the carbon is uniformly distributed on the composite NWs,

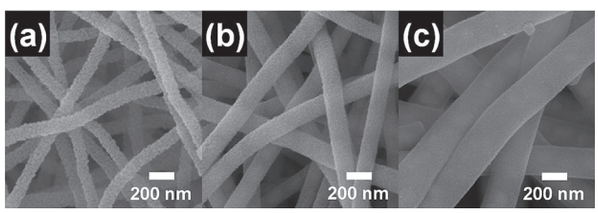

Figure 1. FESEM images of (a) bare SnO_2 NWs, (b) SnO_2–Co_3O_4 composite NWs and (c) carbon-coated SnO_2–Co_3O_4 composite NWs.

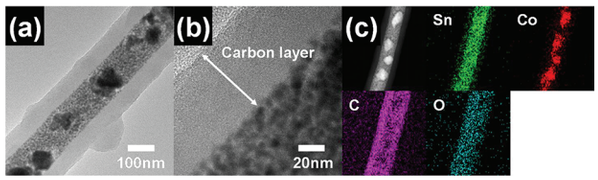

Figure 2. (a) Low-resolution TEM image, (b) high-resolution TEM image and (c) TEM-EDS mapping data obtained from carbon-coated SnO_2–Co_3O_4 composite NWs.

demonstrating the successful formation of carbon-coated SnO_2–Co_3O_4 composite NWs.

Figure 3 shows XRD patterns obtained from all samples. The characteristic diffraction peaks of bare SnO_2 NWs are observed at 26.6°, 33.9°, 37.9°, 51.8° and 54.7°, corresponding respectively to (110), (101), (200), (211) and (220) planes of cassiterite SnO_2 phases with a tetragonal rutile structure (space group $P4_2/mnm$ [136]; JCPDS card No. 21–1250). SnO_2–Co_3O_4 composite NWs show, in addition to the SnO_2 phases, peaks at 31.2°, 36.9° and 44.7°, which are indexed to the (220), (311) and (400) planes, respectively, of spinel Co_3O_4 phases with a face-centered cubic structure (space group Fd3m [227]; (JCPDS card No. 04–0802). For carbon-coated SnO_2–Co_3O_4 composite NWs, in addition to the SnO_2 and Co_3O_4 phases, peaks corresponding to the (011), (002) and (200) plane of SnO phases (JCPDS card No. 72–2324) are observed. In this connection, partial reduction of carbon-coated SnO_2–Co_3O_4 composite NWs is generated by a carbothermal reaction during carbonization.[4] In addition, peaks from the SnO_2 phases in SnO_2–Co_3O_4 composite NWs are broader than those of bare SnO_2 NWs. Generally, the grain size (D) can be explained by using the Scherrer formula:[9]

$$D = 0.9\lambda/(\beta \cdot \cos\theta) \quad (1)$$

where λ, β and θ are the X-ray wavelength, full width at half maximum (FWHM) and the Bragg angle, respectively. Thus, the calculated grain sizes, based on the (110), (101) and (211) planes, are ~10.6 nm for bare SnO_2 NWs, ~6.4 nm for SnO_2–Co_3O_4 composite NWs and ~6.5 nm for carbon-coated SnO_2–Co_3O_4 composite NWs. This reduced grain size of SnO_2 results from co-existence of the SnO_2 and Co_3O_4 phases in the NWs.[13, 14]

Figures 4(a–d) show the XPS spectra obtained from SnO_2–Co_3O_4 composite NWs and carbon-coated SnO_2–Co_3O_4 composite NWs. The XPS Sn 3*d* peaks of the SnO_2–Co_3O_4 composite NWs shown in Figure 4(a) are located at ~486.6 eV for Sn $3d_{5/2}$ and ~495.0 eV for Sn $3d_{3/2}$, which indicates that elemental Sn exists in the SnO_2 phases.[15] The XPS spectra corresponding to Co $2p_{3/2}$ and Co $2p_{1/2}$ are divided into two peaks, as shown in Figure 4(b). The main XPS peaks of Co $2p_{3/2}$ and Co $2p_{1/2}$ are observed at ~780.4 eV and ~795.9 eV whereas the extra peaks are observed at ~785.7 eV and ~802.6 eV, respectively. These results correspond to the formation of the Co_3O_4 phases as previously reported.[16] For the carbon-coated SnO_2–Co_3O_4 composite NWs, while the XPS Sn 3*d* peaks are clearly detected, the XPS Co 2*p* peaks are not observed because of the formation of the carbon layer. The reason is that the Co_3O_4 phases are mainly formed inside the composite NWs as shown in Figure 2(c). In Figure 4(c), the XPS Sn 3*d* peaks are composed of four peaks. That is, the XPS Sn $3d_{5/2}$ and Sn $3d_{3/2}$ spectra are attributed to the main peaks positioned at ~486.7 eV and ~495.1 eV, respectively, that correspond to the SnO_2 phases and the minor peaks positioned at ~486.0 eV and ~494.5 eV, respectively, that correspond to SnO phases, which are in good agreement with the XRD results.[17] The XPS C 1*s* spectra are fitted to three different peaks relative to ~284.4 eV, ~286.0 eV, and ~288.5 eV as shown in Figure 4(d), implying the existence of the C–C, C–N, and C═O binding states, respectively.[18] It is noted that the C–C binding state of the carbon-coated SnO_2–Co_3O_4

Delivered by Ingenta to: Universitat Oviedo
IP: 179.61.201.60 On: Wed, 14 Dec 2016 16:45:14
Copyright: American Scientific Publishers

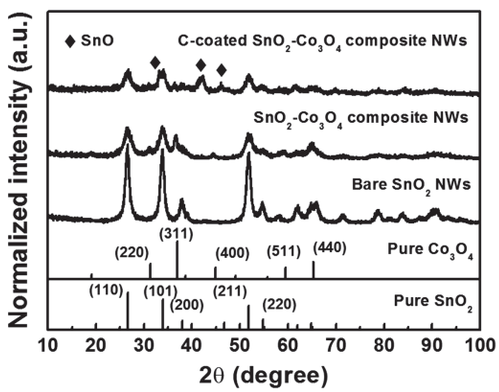

Figure 3. XRD data obtained from all samples.

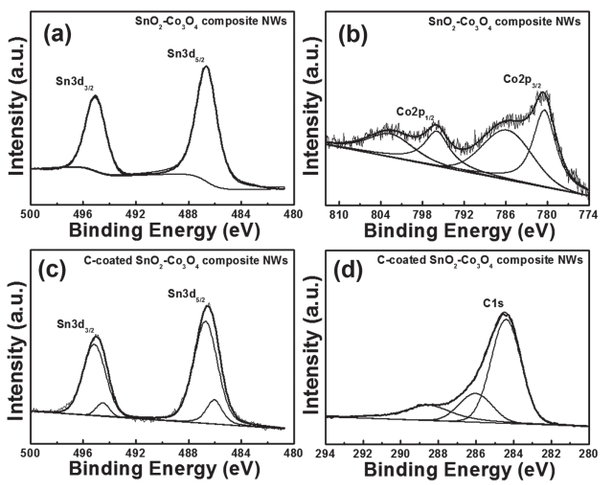

Figure 4. XPS spectra obtained from Sn 3*d* (a) and Co 2*p* (b) of SnO_2–Co_3O_4 composite NWs and Sn 3*d* (c) and C 1*s* (d) of carbon-coated SnO_2–Co_3O_4 composite NWs.

composite NWs (~61.97%) is higher in value compared to that of the SnO_2–Co_3O_4 composite NWs (~47.79%), implying the formation of the carbon layer on composite NWs. Thus, the SEM, TEM, XRD and XPS results demonstrated the successful formation of carbon-coated SnO_2–Co_3O_4 composite NWs.

Figures 5(a–c) display the charge–discharge voltage profiles of all samples, for voltages between 0.01 and 2.0 V, at a current rate of 100 mA/g for various cycle numbers up to 50th. In Figure 4(a), bare SnO_2 NWs show defined voltage plateaus at ~0.9 V in the first discharge process, which is an irreversible reduction of SnO_2 to form amorphous Li_2O and metallic Sn (Eq. (2)).[2] During the first discharge, the Li_2O formed corresponds to electrochemically inactive phases, leading to a large irreversible capacity. An additional cause of large irreversible capacity during first discharge is formation of an irreversible solid electrolyte interface (SEI) layer on the electrodes.[13] After the voltage plateaus, the voltage drops continuously to 0.01 V. This reaction leads to the formation of Li–Sn alloys.[3,9] In addition, the voltage steps at ~0.45 V, ~0.6 V and ~1.2 V during charging are related to de-alloying of Li–Sn. In successive cycles, alloying and de-alloying between Sn and Li^+ (Eq. (3)) occurs reversibly. The reactions can be summarized:[3,4]

$$SnO_2 + 4Li^+ + 4e^- \rightarrow Sn + 2Li_2O \quad (2)$$

$$Sn + xLi^+ + xe^- \leftrightarrow Li_xSn \quad (0 \leq x \leq 4.4) \quad (3)$$

Delivered by Ingenta to [illegible] IP: [illegible] On: Wed, [illegible] Copyright: American Scientific Publishers

Furthermore, the initial discharge capacities are ~2210 mAh/g for bare SnO_2 NWs, ~2000 mAh/g for SnO_2–Co_3O_4 composite NWs and ~1695 mAh/g for carbon-coated SnO_2–Co_3O_4 composite NWs. The differences between initial discharge capacities are attributable to the Co_3O_4 and carbon phases. In general, the Co_3O_4 de-alloying reaction with Li^+ does not appear in the voltage range 0.01–2.0 V, as its oxidation reaction occurs at ~2.1 V.[19] Hence, the initial discharge capacity of SnO_2–Co_3O_4 composite NWs is lower than that of bare SnO_2 NWs. In particular, carbon-coated SnO_2–Co_3O_4 composite NWs exhibit the lowest initial discharge capacity, since carbon possesses much low capacity (372 mAh/g) than SnO_2 (781 mAh/g) and Co_3O_4 (890 mAh/g).[1,4,15] In spite of disadvantages such as low discharge capacity, LIB cells fabricated with carbon-coated SnO_2–Co_3O_4 composite NWs exhibit relatively high reversible capacity up to 50 cycles. Figure 4(d) shows the cycle number dependence of the charge–discharge capacity of the fabricated LIB cells. Up to 50 cycles, the reversible capacity with bare SnO_2 NWs decreases continuously to ~101 mAh/g, which is due to the large volume expansion-contraction of SnO_2 grains during alloying and de-alloying with Li^+.[3,4] In contrast, the reversible capacity of SnO_2–Co_3O_4 composite NWs decreases slowly to ~323 mAh/g. This implies that the composite structure provides improved reversible capacity because reduced grain size of SnO_2 minimizes volume expansion and pulverization of electrodes.[13,20] Furthermore, carbon-coated SnO_2–Co_3O_4 composite NWs exhibit superior reversible capacity (~542 mAh/g after 50 cycle), implying excellent cycle performance. The performance improvement can be explained by two combined effects: first, the composite structure of SnO_2 and Co_3O_4 alleviates the volumetric change of electrode materials.[13,20] Second, the carbon shell acts as a structural buffering layer to alleviate large volume expansion-contraction during alloying and de-alloying of Li^+.[3,4] Thus, the novel electrode design containing NWs with SnO_2–Co_3O_4 composite in their core region and carbon coating in the shell region can offer improved cycle performance for high-performance LIBs.

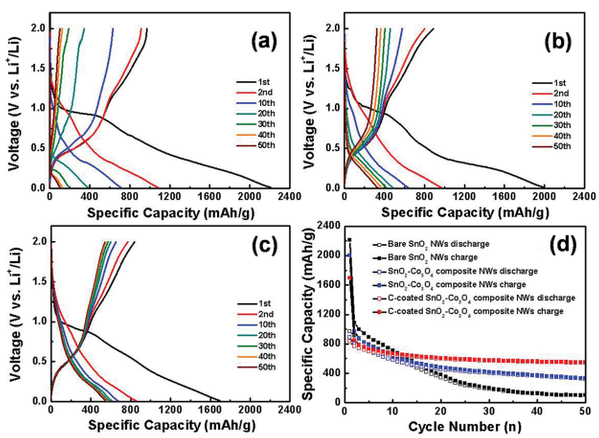

Figure 5. (a–c) Charge–discharge voltage profiles of all samples characterized at a current density of 100 mAh/g in the voltage range of 0.01–2.0 V for various cycle numbers up to 50th. (d) Cycling performance obtained from all samples up to 50 cycles.

4. CONCLUSION

Carbon-coated SnO_2–Co_3O_4 composite NWs were synthesized by electrospinning and carbonization using a dopamine precursor. They exhibited excellent capacity retention compared to bare SnO_2 and SnO_2–Co_3O_4 composite NWs. The results indicate that improved electrochemical performance can be explained as the combined effects of the composite structure of SnO_2–CO_3O_4 and the introduction of a carbon coating that hinders large volume expansion-contraction of the electrodes. Therefore, carbon-coated SnO_2–Co_3O_4 composite NWs should be used as an alternative candidate for anode in high-performance LIBs.

Acknowledgments: This research was supported by Basic Science Research Program through the National Research Foundation of Korea (NRF) funded by the Ministry of Education, ICT and Future Planning (NRF-2015R1A1A1A05001252).

References and Notes

1. S. Goriparti, E. Miele, F. D. Angelis, E. D. Fabrizio, R. P. Zaccaria, and C. Capiglia, *J. Power Sources* 257, 421 (**2014**).
2. H. K. Liu, G. X. Wang, Z. Guo, J. Wang, and K. Konstantinov, *J. Nanosci. Nanotechnol.* 6, 1 (**2006**).
3. Y.-H. Sun, P.-P. Dong, X. Lang, H.-Y. Chen, and J.-M. Nan, *J. Nanosci. Nanotechnol.* 15, 5880 (**2015**).
4. P. Wu, N. Du, H. Zhang, J. Yu, Y. Qi, and D. Yang, *Nanoscale* 3, 746 (**2011**).
5. W.-J. Zhang, *J. Power Sources* 196, 13 (**2011**).
6. Z. Zhou, X. Gao, J. Yan, D. Song, and M. Morinaga, *carbon* 42, 2677 (**2004**).
7. M.-S. Park, G.-X. Wang, Y.-M. Kang, D. Wexler, S.-X. Dou, and H.-K. Liu, *Angew. Chem.* 119, 764 (**2007**).
8. T.-J. Kim, D. Son, J. Cho, B. Park, and H. Yang, *Electrochim. Acta* 49, 4405 (**2004**).
9. S. H. Choi and Y. C. Kang, *Nanoscale* 5, 4662 (**2013**).
10. C. Lei, F. Han, D. Li, W.-C. Li, Q. Sun, X.-Q. Zhang, and A.-H. Lu, *Nanoscale* 5, 1168 (**2013**).
11. G.-H. An, S.-J. Kim, K.-W. Park, and H.-J. Ahn, *ECS Solid State Lett.* 3, M21 (**2014**).
12. C. Wang, X. Wang, B.-Q. Xu, J. Zhao, B. Mai, P. Peng, G. Sheng, and J. Fu, *J. Photochem. Photobiol. A: Chem.* 168, 47 (**2004**).
13. D. Kim, D. Lee, J. Kim, and J. Moon, *ACS Appl. Mater. Interfaces* 4, 5408 (**2012**).
14. U.-S. Choi, G. Sakai, K. Shimanoe, and N. Yamazoe, *Sens. Actuators B* 98, 166 (**2004**).
15. B.-R. Koo, B. K. Park, C. Y. Kim, S.-T. Oh, and H.-J. Ahn, *J. Nanosci. Nanotechnol.* 13, 7590 (**2013**).
16. Z. Ren, Y. Guo, Z. Zhang, C. Liu, and P.-X. Gao, *J. Mater. Chem. A* 1, 9897 (**2013**).
17. L. Y. Liang, Z. M. Liu, H. T. Cao, and X. Q. Pan, *ACS Appl. Mater. Interfaces* 2, 1060 (**2010**).
18. A. Azioune, A. B. Slimane, L. A. Hamou, A. Pleuvy, M. M. Chehimi, C. Perruchot, and S. P. Armes, *Langmuir* 20, 3350 (**2004**).
19. G.-H. An and H.-J. Ahn, *J. Power Sources* 272, 828 (**2014**).
20. H.-J. Ahn, Y.-S. Kim, K.-W. Park, and T.-Y. Seong, *Chem. Commun.* 43 (**2005**), DOI: 10.1039/b407264b.

Received: 17 July 2015. Accepted: 25 March 2016.

Delivered by Ingenta to: Universiteit Utrecht
IP: 179.61.201.60 On: Wed, 16 Nov 2016 04:46:14
Copyright: American Scientific Publishers